Journal of King Saud University – Science 34 (2022) 101792

Contents lists available at ScienceDirect

Journal of King Saud University – Science

journal homepage: www.sciencedirect.com

Original article

Multifactorial antioxidant potential of novel compounds isolated from *Zanthoxylum armatum* fruits along with cytotoxicity studies on HepG2 cell lines

Ateeque Ahmad [a], Sudeep Tandon [a], Heena Tabassum [b,c], Zulfa Nooreen [a,*], Iffat Zareen Ahmad [c], Ulrike Lindequist [d], Ramzi A. Mothana [e], Perwez Alam [e], Nasir Ali Siddiqui [e,*]

[a] Department of Phytochemical Technology, Central Institute of Medicinal and Aromatic Plants, Lucknow, 226015, India
[b] Dr. D. Y. Patil Biotechnology and Bioinformatics Institute, Dr. D. Y. Patil Vidyapeeth, Pune, Pune, 411 033, India
[c] Natural Products Laboratory, Department of Bioengineering, Integral University, Dasauli, Kursi Road, Lucknow 226026, India
[d] Department of Pharmaceutical Biology, Institute of Pharmacy, Ernst-Moritz-Arndt-University, Greifswald, F-L-Jahnstr. 17, D-17487, Greifswald, Germany
[e] Department of Pharmacognosy, College of Pharmacy, King Saud University, Riyadh 11451, Saudi Arabia

ARTICLE INFO

Article history:
Received 7 October 2021
Revised 18 November 2021
Accepted 20 December 2021
Available online 27 December 2021

Keywords:
Zanthoxylum armatum
Rutaceae
Fruits
New compounds
Cytotoxic
Antioxidant

ABSTRACT

Objective: Oxidative stress causes multidirectional damage including different types of cancers in our body by affecting the normal physiological functions of the cells and tissues. The objective is to study the cytotoxic and antioxidant potential of natural compounds isolated from fruits of *Z. armatum* DC.
Methods: This study was designed to investigate the chemical nature as well as biological effects of natural compounds. The isolated compounds were tested for antioxidant effect in various ways e.g. DPPH free radical inhibition, ferric reducing effect, superoxide dismutase, and catalase evaluation. The cytotoxic effect of isolated compounds was evaluated using HepG2 cancer cells.
Results: Chemical investigations on the fruits of *Z. armatum* DC, led to the isolation of two new compounds characterized as (*cis*)-2, 8-dimethyl-non-5-en-8-ol-2-olyl benzoate (**1**), (*cis*)-2, 10-dimethyl-undec-7-en-10-ol-2-olyl benzoate (**2**) along with five known compounds such as *n*-dodecanyl linoleniate (**3**), *n*-octacos-10, 20-dienoic acid (**4**), (*cis*, *cis*)-dotriacont-6, 12-dienoic acid (**5**), lignoceric acid (**6**), and (*cis*, *cis*)-dotriacont-6, 8-dienoic acid (**7**). Compound **1** shows potent activity against HepG2 cancer cells in comparison **2** and significantly affected the viability of cells till 48 hrs. The highest antioxidant potential among compounds and extracts with respect to DPPH free radical inhibition and the ferric reducing effect was shown by compound **1** followed by **2** and **7** with an EC50 value of 19.44, 20.44 and, 22.46 respectively.
Conclusions: The present study indicates that compound (1) showed a significant effect against HepG2 cancer cells as well as antioxidant potential through DPPH and FRAP methods. Compounds 2 and 7 also proved to be useful up to some extent for antioxidant potential.

1. Introduction

Aromatic tree or large shrub of *Zanthoxylum armatum* Timur commonly known as prickly ash is an important medicinal plant. Its fruits contain single rounded and shining black seeds, 2–3 mm in size, found in four hot valleys of subtropical to the temperate Himalayas of North-East India and Pakistan, Laos, Myanmar, Thailand, China (Phuyal et al., 2018). It has been traditionally used in the treatment of various diseases such as hypertension, abdominal pain, fever, high altitude sickness, diarrhea, and as a tonic, condiment, and anthelmintic treatment (Mushtaq et al., 2019). Fruits are used for the treatment of toothache, stomachache, dys-

Abbreviations: CAT, Catalsase; SOD, Superoxide dismutase; FRAP, Ferric reducing antioxidant power; ROS, Reactive oxygen species; DPPH, 1,1-diphenyl-2-picrylhydrazyl; NMR, Nuclear magnetic resonance.

* Corresponding authors at: Phytochemical Technology Depatment, Central Institute of Medicinal and Aromatic Plants, Lucknow 226016, India.
E-mail addresses: khan.zulfanooreen7860@gmail.com (Z. Nooreen), nsiddiqui@ksu.edu.sa (N.A. Siddiqui).

Peer review under responsibility of King Saud University.

Production and hosting by Elsevier

https://doi.org/10.1016/j.jksus.2021.101792
1018-3647/

pepsia, and as a carminative. Seeds are used for condiments and flavoring agents. Young shoots as toothbrushes and are useful for curing gum diseases (Abbasi et al, 2010). The fruits extract is effective in expelling roundworms, due to its deodorant, disinfectant, and antiseptic properties, the fruits are also used in case of dental troubles (Gaur, 1999). Toothache tree or *Z. armatum* plays an important role in the history of the Indian system of medicines also and its volatile oil possesses active constituents such as linalool, limonene, and lignan. Various studies indicated that it possesses larvicidal, antifungal, hepatoprotective, and allelopathic properties (Singh and Singh, 2011). According to Ayurveda it has been used in swassa, kasa, Ardita, Danta roga, hrdroga, and many more diseases (Anonymous, 2004).

Phytochemical constituents such as alkaloids, sterols, phenolics, lignans, coumarins, terpenoids, flavonoids, and their glycosides and others have been isolated from the plant. Armatamide (1)-, asarinin and fargesin, alpha- and beta-amyrins, lupeol, and beta-s itosterol-beta-D-glucoside-have been isolated from the bark of *Zanthoxylum armatum* (Kalia et al., 1999), and tambulin, prudomestin, ombuin and 3, 4, 5, 3′, 4′, 5′-hexahydroxydiphenyl ether (Nooreen et al., 2017 A) and 2α-methyl-2β-ethylene-3β-isopropyl-cyclohexan-1β, 3α-diol and phenol-*O*-β-D-arabinopyra nosyl-4′-(3″,7″,11″,15″-tetramethyl)-hexadecan-1″-oate, *m*-methoxy palmityloxy benzene, acetyl phenyl acetate, linoleiyl-*O*-α-D-xylopyranoside, *m*-hydroxyphenoxy benzene and palmitic acid have been isolated from the hexane extract of fruits (Nooreen et al., 2017b) (*7S,8R*)-guaiacylglycerol-ferulic acid ether-7-O-β-D-glucopyranoside, *erythro*-1-(4-hydroxyphenyl) glycerol, *thero*-syringylglycerol, *erythro*-syringylglycerol, 7-(3-hydroxy-5-methoxyphenyl) propane-7,8,9-triol, *threo*-guaiacylglycerol, (−)-(*7R,8S*)-guaiacylglycerol 8-O-β-d-glucopyranoside, xylocoside A, syringing, coniferin, 3-hydroxy-2-{4-[(1E)-3-hydroxyprop-1-en-1-yl]-2-methoxyphenoxy}propyl-d-glucopyranoside, psoralenoside are also reported from *Z. armatum* fruits (Guo et al., 2017).

2. Material and methods

2.1. Instruments, chemicals and reagents

Melting points were determined using digital melting point apparatus (Sonar) India, whereas Rudolf autopol model polarimeter measured the optical rotations. The solvents, hexane, ethyl acetate, methanol, ethanol, glacial acetic acid, sulphuric acid, hydrochloric acid, were purchased from E-Merck Ltd, India. Precoated TLC plates (layer thickness 0.25 mm), silica gel for column chromatography (70–230 mesh ASTM) and LiChroprep RP-18 (40–63 μm) were from Merck (Germany). Authentic standards of chemicals were purchased from Sigma-Aldrich (USA). Ultraviolet–visible spectroscopy was measured with TU-1800$_{PC}$ UV–vis spectrophotometer. Both ^{1}H and ^{13}C NMR spectra were recorded in $CDCl_3$ and CD_3OD on a Bruker DRX-300 & 500 model spectrometers operating at 300 and 75 and 500 and 125 MHz, respectively. NMR spectra were obtained in deuterated chloroform, methanol using tetramethylsilane (TMS) as an internal standard, FAB-MS data were recorded on a JEOL SX-102 spectrometer, and Electrospray ionization (ESI) mass spectra were recorded in positive mode on an API-3000, LC/MS/MS (Applied Biosystem/MDS SCIEX, Toronto, Canada) mass spectrometer using a standard ESI source coupled with LC separation system and HR ESI MS in the positive mode was recorded on an agilent 6520 QTOF (ESI-HRMS). Infrared spectroscopy was recorded on an FT-IR spectrophotometer Shimadzu 8201 PC (4000–400 cm^{-1}). Thin layer chromatography was performed on precoated silica gel 60 F_{254}, plates (Merck, layer thickness 0.25 mm). Visualization of the TLC spots was performed using 5% H_2SO_4 in ethanol spray reagent.

2.2. Plant material

The fruits of *Z. armatum* were purchased from the local market of Lucknow, State of Uttar Pradesh, India in the month of March 2018 and identified by the Department of Botany and Pharmacognosy, CIMAP. A voucher specimen (ZA/F/14) was deposited in the herbarium of the CSIR-CIMAP, India**.**

2.3. Extraction of fruits

Dried fruits of *Z. armatum* (14.5 Kg) in powdered form were extracted with methanol (70 L) by refluxing 8 h for three days and concentrated *in vacuo* to obtain a semisolid brown mass to yield (2.9 kg) of an extract, which was suspended in water and extracted with hexane, ethyl acetate and, *n*-butanol, successively, to produce 1.5 kg, 300 g, 258 g and, 603 g extracts, respectively. Isolated compounds (1–7), ethyl acetate fraction (8), and *n*-butanol fraction (9) was evaluated for cytotoxicity and antioxidant potential.

2.4. Isolation of the compounds from ethyl acetate extract of Z. armatum

The ethyl acetate extract (206 g) was subjected to silica gel column (1.5 kg; 60–120 mesh size) and eluted with solvent of *n*-hexane, *n*-hexane-EtOAc (9:1–1:9, v/v), EtOAc, and MeOH to give 37 fractions (frs.; each of 10 L). Fractions were checked by TLC and showing complex mixtures, fraction 7 (11 g, *n*-hexane-EtOAc 7:3) were chromatographed over silica gel column (90 g; 60–120 mesh size, each fraction of 50 ml) yields. The elution was sequentially performed with $CHCl_3$, $CHCl_3$-MeOH (9.5:0.5, 9:1, 8:2 v/v) Compound **1 (10 mg),** fraction 26 (3.4 g, obtained in EtOAc) were re-chromatographed over silica gel column (50 g; 200–400 mesh size; each fraction of 20 ml). The elution was sequentially performed with $CHCl_3$, $CHCl_3$-MeOH (1%, 2%, 3%, 4%, 5% v/v) to yield 20 fractions yield Compound **2 (25 mg)**.

Fraction I (105 gm) was subjected to silica gel column (500 gm; 60–120 mesh size) and eluted with solvent of *n*-hexane, *n*-hexane-EtOAc (1:1, 3:7, 2:8, 1:9 v/v), EtOAc, and MeOH to give 17 fractions (each of 15 L). Fraction 2 (25gm, *n*-hexane-EtOAc 1:1) was chromatographed over silica gel column (50 g; 60–120 mesh size, each fraction of 20 ml) elution was sequentially performed with $CHCl_3$, $CHCl_3$-MeOH (0.5%, v/v) yields 10 fractions yield Compound **3 (10 mg)**. Fraction 7&8 (41 g, *n*-hexane-EtOAc 7:3) were chromatographed over silica gel column (120 g; 60–120 mesh size, each fraction of 100 ml). The elution was sequentially performed with $CHCl_3$, $CHCl_3$-MeOH (1%, 2%, 5% v/v) to yields 25 fractions yields Compound **5 (15.2 mg),** Compound **6 (20 mg),** Fraction 13&14 (20 g, *n*-hexane-EtOAc 9:1) were chromatographed over silica gel column (100 g; 60–120 mesh size, each fraction of 50 ml) and elution was sequentially performed with $CHCl_3$, $CHCl_3$-MeOH (0.5%, 1%, 2%, 3%, v/v) to yield 12 fractions yields Compound **4 (22 mg),** and the isolation of Compound **7** from the method described by Nooreen et al. (2017a).

2.4.1. ***Compound 1:****(cis)-2, 8-dimethyl-non-5-en-8-ol-2-olyl benzoate*

Semi-solid, R_f 0.47($CHCl_3$:MeOH; 9.5:0.5); UV λ_{max}(MeOH): 256, 266, 277; IRν_{max} (KBr): 3403, 2926, 2856, 1721, 1633, 1548, 1435, 1377, 1177, 1015, 931 cm^{-1}; ^{1}H NMR (MeOD; 500 MHz): δ 6.71 (1H, m, H-4′), 5.99 (1H, m, H-2′), 5.96 (1H, m, H-6′), 5.94 (1H, ddd, *J* = 1.5, 3.0, 8.5 Hz, H-5), 5.92 (1H, ddd, *J* = 1.5, 1.5, 8.6 Hz, H-6), 5.59 (1H, m, H-3′), 5.56 (1H, m, H-5′), 3.23 (2H, m, H_2-4), 2.2. (2H, m, H_2-3), 1.67 (2H, d, *J* = 7.5 Hz, H_2-7), 1.09 (12H, s, Me-

1), Me-9, Me-10, Me-11); ^{13}C NMR ($CDCl_3$; 125 MHz): δ 18.48 (C-1), 71.78 (C-2), 33.10 (C-3), 32.70 (C-4), 125.18 (C-5), 129.93 (C-6), 51.22 (C-7), 71.78 (C-8),27.36 (C-9), 18.48 (C-10), 27.36 (C-11), 145.29 (C-1′), 132.98 (C-2′), 133.25 (C-3′), 131.60 (C-4′), 133.25 (C-5′), 132.82 (C-6′), 169.20 (C-7′); ESIMS *m/z* (rel. int.): 291 $[M+H]^+$, ($C_{18}H_{27}O_3$) (10.2), 245 (8.4); HR-ESI/MS *m/z* 291.1968 $[M+H]^+$ (calcd. 291.1960 for ($C_{18}H_{27}O_3$).

2.4.2. ***Compound 2:****(cis)-2, 10-Dimethyl-undec-7-en-10-ol-2-olyl benzoate*

Semi-solid, R_f 0.34 ($CHCl_3$:MeOH; 9.5:0.5); UV λ_{max} (MeOH): 266 nm; IR ν_{max} (KBr): 3415, 2974, 2928, 1725, 1630, 1550, 1440, 1363, 1258, 1175, 993, 906 cn-1; ^{1}H NMR ($CDCl_3$; 500 MHz$_)$): δ 6.78 (1H, m, H-4′), 6.05 (1H, m, H-2′), 6.01 (1H, m, H-6′), 5.83 (1H, m, H-3′), 5.80 (1H, m, H-5′), 5.67 (1H, ddd, *J* = 2.5, 7.0, 7.5 Hz, H-8), 5.63 (1H, ddd, *J* = 8.0, 5.5, 7.6 Hz, H-7), 3.24 (2H, m, H_2-6), 2.58 (2H, m, H_2-3), 2.29 (2H, m, H_2-4), 2.21 (2H, m, H_2-5), 1.72 (2H, d, *J* = 7.0 Hz, H_2-9), 1.16 (12H, s, Me-1, Me-11, Me-12, Me-13); ^{13}C NMR ($CDCl_3$; 125 MHz): δ 18.20 (C-1), 70.80 (C-2), 32.06 (C-3), 31.87 (C-4), 31.82 (C-5), 31.34 (C-6), 123.60 (C-7), 129.36 (C-8), 50.19 (C-9), 70.80 (C-10), 27.11 (C-11), 26.42 (C-12), 18.26 (C-13), 144.34 (C-1′), 132.01 (C-2′), 131.53 (C-3′), 130.04 (C-4′), 131.39 (C-5′), 131.61 (C-6′, 167.27 (C-7′); ESIMS *m/z* (rel. int.): 319 $[M+H]^+$ ($C_{20}H_{31}O_3$) (70.4); HR-ESI/MS *m/z* 319.2278 $[M+H]^+$ (calcd. 319.2273 for $C_{20}H_{31}O_3$).

2.5. Cell viability study on HepG2 cells

The HepG2 (Liver) and lung (A549) cancer cell lines were obtained from the German Collection of Moicroorganisms and Cell Cultures (DSMZ), Braunschweig, Germany. The cell viability of isolated compounds (**1–7),** ethyl acetate extract and, *n*-butanol extract was tested using a protocol of Fraga et al. (2008) with slight modifications, and this assay was used to detect the influence of isolated compounds on cell viability using the following protocol (Fraga et al., 2008). The effect of different compounds on the viability of normal and transformed cells was determined by MTT (3- [4, 5-dimethylthiazol-2-yl]-2, 5-diphenyltetrazolium bromide) assay. Briefly, cells were seeded in a 96-well plate at a density of 1×10^4 cells/well. Cells were treated with different concentrations of samples (10 μg, 20 μg, 30 μg, 40 μg, 50 μg, 100 μg, 150 μg, and 200 μg) at 24 h, 48 h, and 72 h to determine the toxic and sub-toxic doses. At the end of treatment, 20 μL MTT (5 mg/mL) was added to each well. After incubation for 3 h, media along with MTT was removed. 200 μL DMSO was added to dissolve the formazan crystal, and absorbance was recorded at 540 nm using an ELISA plate reader. The plot of percent cell viability versus different compounds concentrations was used to calculate the concentration lethal to 50% of the cells (IC_{50}). The cellular morphological changes were observed under inverted phase-contrast microscopy (Nikon Eclipse Ti-S, Tokyo, Japan). A similar test of different compounds was also performed on WRL-68 to examine if the treatment had a distinguishable effect between normal and cancer cells.

2.6. Quantification of intracellular reactive oxygen species (ROS)

Intracellular reactive oxygen species **(**ROS) generation was analyzed by using fluorescence microscopic imaging technique as per previous protocol (Siddiqui, 2015). Cells (1×10^4 per well) were exposed with compound 1with sub IC_{50} value and IC_{50} value, i.e., 25.375 μg/ml and 50.75 μg/ml for 24 h and 48 h. Subsequently, cells were incubated with Dichloro-dihydro-fluorescein diacetate (DCFH-DA, 10 mM) at 37 °C for 30 min and washed with PBS. The intracellular fluorescence intensity of cells was visualized by an inverted fluorescence microscope (Nikon ECLIPSE Ti-S, Tokyo, Japan). For quantitative fluorometric analysis, cells (1×10^4per well) were seeded and treated with different compounds in 96-well black bottom culture plate. Fluorescence intensity was measured with a multiwall microplate reader (Synergy H1 Hybrid Multi-Mode Microplate Reader, BioTek, Winooski, VT) at an excitation wavelength of 485 nm and an emission wavelength of 528 nm. ROS production was quantified using Image J software (Image J, National Institutes of Health, and Bethesda, MD). Data were expressed as a percentage of fluorescence intensity relative to the control wells.

2.7. DPPH radical inhibition activity

The free radical inhibition activity of different compounds (1–7), ethyl acetate extract (8), and butanol extract (9) were determined by 1, 1-diphenyl-2-picrylhydrazyl (DPPH Assay) (Blois, 1958). 3 ml reaction mixture was prepared which contained different concentrations of the crude extract and 0.1 mM methanolic DPPH solution and was incubated for 30 min. The absorbance of each reaction mixture using a spectrophotometer was taken at 517 nm where lower absorbance recorded for the reaction mixture indicated elevated free radical inhibition activity. All extracts were analyzed in triplicates. Ascorbic acid was taken as a standard.

$$DPPH\ inhibition\ activity(\%) = (A_0 - A_1/A_0) \times 100$$

Where, A_1- Sample absorbance; A_0 - Absorbance of the control.

2.8. Ferric reducing antioxidant power (FRAP) assay

This assay is based upon the measurement of the change in absorbance at 593 nm occurring due to the development of blue color. A blue-colored ferrous; Fe^{2+} – 1,2,5 tripyridyltriazine compound was formed from the colorless oxidized ferric Fe^{3+} form due to the electron-donating antioxidants (Benzie and Strain, 1996). The FRAP assay solutions consisted of 300 mM acetate buffer pH 3.6, 10 mM, TPTZ (2,4,6- tripyridyltriazine) added in 40 mM HCl and 20 mM $FeCl_3$·6H2O $FeSO_4$ was taken as a standard. Results of percentage scavenging were compared with the standard i.e. Ascorbic acid.

$$FRAP\ scavenging\ activity\ (\%) = (A_0 - A_1/A_0) \times 100$$

Where, A_1- sample absorbance A_0 – absorbance of the control.

2.9. Assay of antioxidant enzyme (SOD and Catalase) activities

The samples containing the antioxidant enzymes to be tested were prepared by the following steps described by Mukherjee and Choudhuri (1983) with some modifications, Samples were finely ground by pestle in an ice-cold motor in 10 ml of phosphate buffer (KH_2PO_4/K_2HPO_4) (100 mM) with pH 7.0, having Na_2EDTA (0.1 mM) and also 0.1 g of polyvinylpyrrolidone (PVP) was added to the samples. Filtering of the homogenate using filter paper was done, centrifuged at 15000Xg for 10 min at 4 °C, the supernatant was re-centrifuged at 18000Xg for 10 min, the supernatant was stored at 4 °C for enzyme assay.

2.9.1. Superoxide dismutase (SOD) activity

To measure the SOD enzyme activity a reaction solution of 3 ml was prepared according to the procedure of Giannopolitis and Ries, 1977. Nitro blue tetrazolium (NBT) was photochemically reduced at 560 nm therefore, the inhibition of photochemical reduction of nitro blue tetrazolium (NBT) at 560 nm was measured which determines SOD activity where an amount of enzyme causing 50% inhibition in the photochemical reduction of NBT was termed as one unit of SOD activity.

2.9.2. Catalase activity

Catalase enzyme (CAT) activity was determined by the method of Aebi et al., in a reaction solution (3 ml). The reduction in the absorbance at 240 nm for 1 min with respect to the H_2O_2 consumption estimated the catalase activity (Aebi, 1984).

2.10. Statistical analysis

All data are expressed as mean ± standard deviation (SD). Statistical analyses were performed using One-way ANOVA. Differences as $p < 0.05$ were considered statistically significant

3. Result

3.1. Characterization of compounds

Compound **1** (Fig. 1), was obtained as yellow semi-solid mass from ethyl acetate extract and its IR spectrum displayed absorption bands for hydroxyl group (3403 cm^{-1}), ester function (1721 cm^{-1}), unsaturation (1633 cm^{-1}), and aliphatic chain (931 cm^{-1}). Its molecular ion peak was determined at *m/z* 291 $[M+H]^+$ on the basis of ESIMS and ^{13}C NMR spectra corresponding to the molecular formula of an aromatic ester with aliphatic chain $C_{18}H_{27}O_3$.

The ^1H NMR spectrum of compound **1**, showed deshielded signals as a triple-doubles at δ 5.94 (J = 1.5, 3.0, 8.5), 5.92 (J = 1.5, 1.5, 8.6 Hz) and multiplets at δ 6.71, 5.99, 5.96, 5.59 and 5.56 were assigned to vinylic H-5, H-6 and aromatic protons H-2′, H-3′, H-4′, H-5′ and H-6′. Twelve three-proton signals as a broad singlet at δ 1.09, as doublets at δ 1.67 (J = 7.5 Hz), and multiplets at δ 2.20, 3.23 were associated with tertiary C-1, 9, 10, 11 methyls, and C-7, 3, 4 methylene protons. The ^{13}C NMR spectrum of **1**, exhibited a signal for ester carbon at δ 169.20 (C-7′), and vinylic carbons appeared at δ 125.18 (C-5), 129.93 (C-6) were assigned. The six aromatic carbons were appeared at δ 145.29 (C-1′), 132.98 (C-2′), 133.25 (C-3′), 131.60 (C-4′), 133.25 (C-5), and 132.82 (C-1′). The methyl and vinylic carbons appeared at δ 18.48 (C-1, 10), 27.36 (C-9, 11) and at δ 125.18 (C-5), 129.93 (C-6), respectively. The methylene and methane carbons were appeared at δ 33.10 (C-3), 32.70 (C-4), 51.22 (C-7), and 71.78 (C-2), 71.78 (C-8), respectively. The presence of C-7′ signal in the deshielded region at δ 169.20, and C-1′ signal also deshielded in at δ 145.29 suggested ketone linkage of the benzene ring.

The ^1H–^1H COSY spectrum of **1** showed correlations of H-2′ with H-3′ and H-4′; H-7 with H-9, 11 methyls and H-6 methine; H-3 with H-1, and 10 methyls. The HSQC experiment of **1** showed key-correlations between the protons H-2′ at δ 5.99 and C-2′ at δ 132.98; H-6′ at δ 5.96 and C-6′ at δ 132.82; H-5 at δ 5.94 and C-5 at δ 128.18; H-6 at δ 5.92 and C-6 at δ 129.93; H-3 at δ 2.20 and C-5 at δ 33.10; H-4 at δ 3.23 and C-4 at δ 32.70; H-7 at δ 1.67 and C-7 at δ 51.22. The HMBC spectrum of **1** exhibited interaction of H-2′, H-3′ and H-6′ with C-1′; H-3′ and H-4′ with C-5′; H-1 and h-10 with C-2; H-4 with C-5 and C-6; H-7 with C-5, C-6, and C-8; H-9, 11 with C-8. On the basis of the evidence of spectroscopic studies, the structure of **1** was established as (*cis*)-2, 8-dimethyl-non-5-en-8-ol-2-olyl benzoate **(1).** This is a new compound and reported the first time in nature.

Compound **2** (Fig. 1), was obtained as yellow semi-solid mass from ethyl acetate extract and its IR spectrum displayed absorption

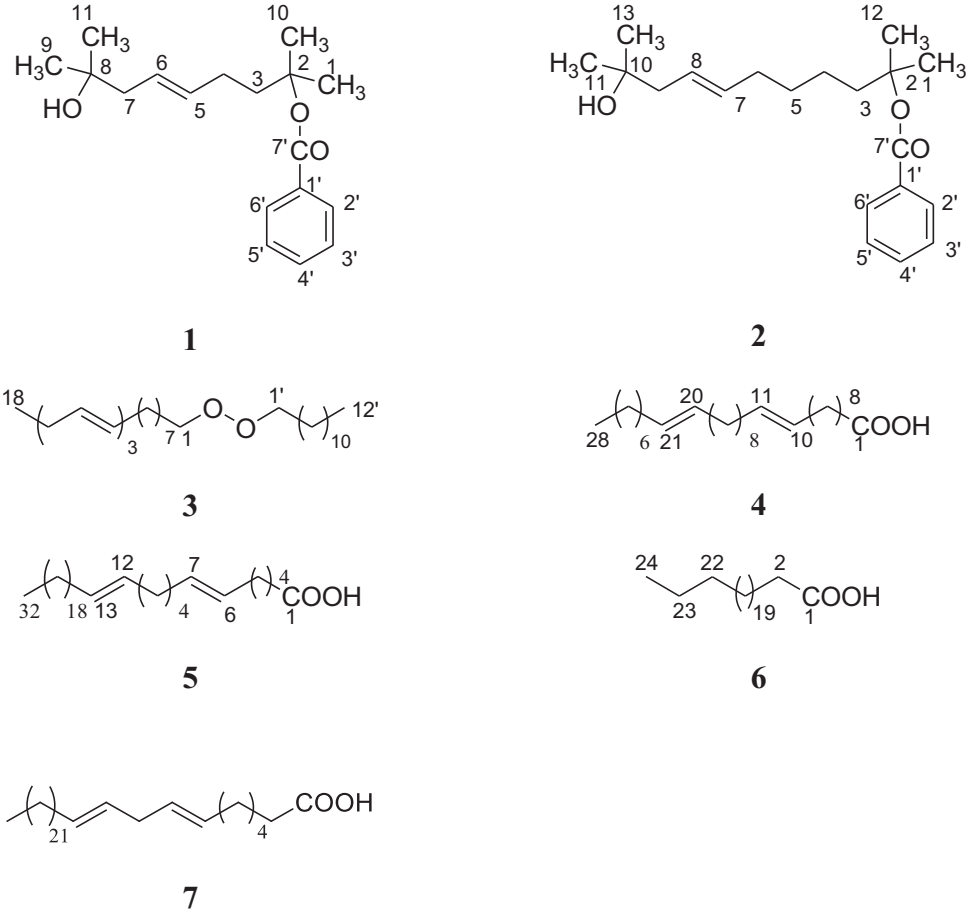

Fig. 1. Chemical structures of compounds (1 – 7) isolated from *Z. aramtum* fruits.

bands for hydroxyl group (3415 cm^{-1}), ester function (1725 cm^{-1}), unsaturation (1630 cm^{-1}), and aliphatic chain (906 cm^{-1}). Its molecular ion peak was determined at *m/z* 319 $[M+H]^+$ ($C_{20}H_{31}O_3$) on the basis of ESIMS and ^{13}C NMR spectra corresponding to the molecular formula of an aromatic ester with an aliphatic chain ($C_{20}H_{31}O_3$).

The ^1H NMR spectrum of compound **1**, showed deshielded signals as a triple doublet at δ 5.67 (J = 2.5, 7.0, 7.5), 5.63 (J = 8.0, 5.5, 7.6 Hz) and multiplets at δ 6.78, 6.05, 6.01, 5.83 and 5.80 were assigned to vinylic H-8, H-7 and aromatic protons H-2′, H-3′, H-4′, H-5′ and H-6′. Twelve three-proton signals as broad singlet at δ 1.16, as doublet at δ 1.72 (J = 7.0 Hz), and multiplets at δ *3.24*, 2.58, 2.29 and 2.21 were associated with tertiary C-1, 11, 12, 13 methyls, C-9, 3–6 methylene protons. The ^{13}C NMR spectrum of **1**, exhibited signals for ester carbon at δ 169.20 (C-7′), vinylic carbons at δ 125.18 (C-5), 129.93 (C-6) and aromatic carbons δ 145.29 (C-1′), 132.98 (C-2′), 133.25 (C-3′), 131.60 (C-4′), 133.25 (C-5) and 132.82 (C-1′).

The ^1H–^1H COSY spectrum of **2** showed correlations of H-2′ with H-3′ and H-4′; H-7 with H-8 and H-6; H-9 with H-11 methyls and H-9 methylene; H-3 with H-1. The HSQC experiment of **1** showed key-correlations between the protons H-2′ at δ 6.05 and C-2′ at δ 132.01; H-6′ at δ 6.01 and C-6′ at δ 131.61; H-7 at δ 5.63 and C-7 at δ 123.60; H-8 at δ 5.67 and C-8 at δ 129.36; H-3 at δ 2.58 and C-3 at δ 32.06; H-4 at δ 2.29 and C-4 at δ 31.87; H-9 at δ 1.72 and C-9 at δ 50.19. The HMBC spectrum of **1** exhibited interaction of H-2′, H-3′ and H-6′ with C-1′; H-3′ and H-4′ with C-5′; H-1 and H-10 with C-2; H-6 with C-7 and C-8; H-9 with C-7, C-8 and C-9; H-11, 13 with C-10. On the basis of these evidences of spectroscopic studies, the structure of **2** was established as (*cis*)-2, 10-dimethyl-undec-7-en-10-ol-2-olyl benzoate (2). This is a new compound and reported the first time in nature.

3.2. Cytotoxicity evaluation

All the isolated compounds (1–7), ethyl acetate extract (8), and butanol extract (9) were evaluated for cytotoxic activity against the growth of HepG2 and A549 cancer cells in a dose-dependent and time-dependent manner using MTT assay to assess cell inhibition. The results are shown in Table 1. Nine treatments (**1** to **9**) were screened by using MTT cell viability assay. Compound **1** was the most potent inhibitor of HepG2 cancer cells compared to compounds 2 and 7. It significantly affected the viability of cells till 48 h. After which there was no effect. The IC_{50} value of **1** was approximately 50 ± 0.05 μg/mL against HepG2 at 24 h. and 25 ± 0.02 μg/mL at 48 hrs against standard drug doxorubicin IC_{50} of 0.95 ± 0.08 μg/mL at 24 hrs and 1.7 ± 0.01 μg/mL at 48hrs against HepG2 cancer cells. A similar IC_{50} value for doxorubicin has been reported by other researchers (Khazaei et al., 2017). Compound 2 and 7 also exhibited a certain degree of cytotoxicity with an IC_{50} value of 52.37 ± 0.04/78 ± 0.02 in 24 hrs/48 hrs and 52.40 ± 0.04 /78 ± 0.02 in 24hrs/48 hrs, respectively.

3.3. Quantification of intracellular reactive oxygen species (ROS) assay

The HepG2 cells treated with compound **1** showed a significant increase in ROS intensity in a dose- and time-dependent manner as compared to untreated cells as shown in Fig. 2. (a) Control cells for 24 h. (b) Cells treated for 24 h with 25.375 μg/mL of compound 1. (c) Cells treated for 24 h with 50.75 μg/mL of **1**. (d) Control cells for 48 h. (e) Cells treated for 48 h with 25.37 μg/mL of compound **1**. (f) Cells treated for 48 h with 50.02 μg/mL of compound 1. The results of the quantitative measurement of ROS showed that 25.37 μg/mL of compound **1** induced a 122.43% increment in ROS production as compared to untreated cells. Moreover, ROS production was increased by 165.53% ($p < 0.001$) at 50.75 μg/mL of compound 1 compared to untreated cells. Those findings are properly supported via previous reports, in which the induction inside the ROS generation was documented because of the effect of herbal bioactive compounds (Karimi et al. 2010; Ghali et al., 2014).

3.4. Antioxidant activity

DPPH free radical inhibition activity of various compounds in various concentrations is depicted in Table 2A, Fig. 3A. The inhibition activity of the different compounds revealed that the highest inhibition was caused by compound **1** followed by **2** and **7** compounds. Inhibition shown by these compounds was far higher than the other compounds and to some extent was comparable to the standard i.e. ascorbic acid over the IC_{50} value 14.90, 15.44, and 15.53 (Table 3, Fig. 4). Compound **5** recorded the least inhibition having an IC_{50} value of 20.61 and the rest tested compounds demonstrated moderate inhibition. Results on Fe (III) reduction demonstrated that all the treated extracts and compounds had lower reducing ability than the radical inhibiting activity (Table 2B). **1**, **2,** and **7** compounds showed the highest reducing ability at an EC_{50} value of 19.44, 20.44, and 22.46 respectively (Table 3). Compounds showed reducing ability which was nearly comparable to the standard used i.e. FeSO4 (Table 3, Fig. 4). The reducing effect of all the compounds increased with an increase in their concentrations. The highest activity of SOD (427.14 ± 0.5 2) was reported for compounds **1**(Table 4, Fig. 5A). In contrary to this a remarkable decrease in SOD enzyme activity was recorded in compound **6** which was 121.11 ± 0.50 (Fig. 3B).

Table 1
Cytotoxicity evaluation on HepG2 and A549 cancer cells of all the samples (*cis*)-2, 8-dimethyl-non-5-en-8-ol-2-olyl benzoate (**1**), (*cis*)-2, 10-dimethyl-undec-7-en-10-ol-2-olyl benzoate (**2**), *n*-dodecanyl linoleniate (**3**), *n*-octacos-10, 20-dienoic acid (**4**), (*cis*, *cis*)-dotriacont-6, 12-dienoic acid (**5**), lignoceric acid (**6**), (*cis*, *cis*)-dotriacont-6, 8- dienoic acid (**7**), ethylacetate extract (8) and butanol extract (9).

Treatment	IC50 values (μg/mL)					
	24 h		48 h	48 h	72 h	72 h
	HepG2	A549	HepG2	A549	HepG2	A549
1	50 ± 0.05	>100	25 ± 0.02	>100	80 ± 0.03	>100
2	52.37 ± 0.04	>100	78 ± 0.02	>100	75 ± 0.02	>100
3	80.39 ± 0.039	>100	80.39 ± 0.039	>100	84.39 ± 0.039	>100
4	54.83 ± 0.01	>100	80 ± 0.07	>100	76 ± 0.03	>100
5	82.39 ± 0.05	>100	84.39 ± 0.05	>100	84.39 ± 0.05	>100
6	86.00 ± 0.07	>100	98 ± 0.01	>100	95 ± 0.06	>100
7	52.40 ± 0.04	>100	78 ± 0.02	>100	75 ± 0.02	>100
8	57.07 ± 0.02	>100	45 ± 0.02	>100	42 ± 0.03	>100
9	54.60 ± 0.06	>100	55.60 ± 0.06	>100	60.60 ± 0.06	>100
Doxorubicin (Std.)	0.95 ± 0.08	0.85 ± 0.03	1.7 ± 0.01	0.65 ± 0.02	0.2 ± 0.03	0.55 ± 0.03

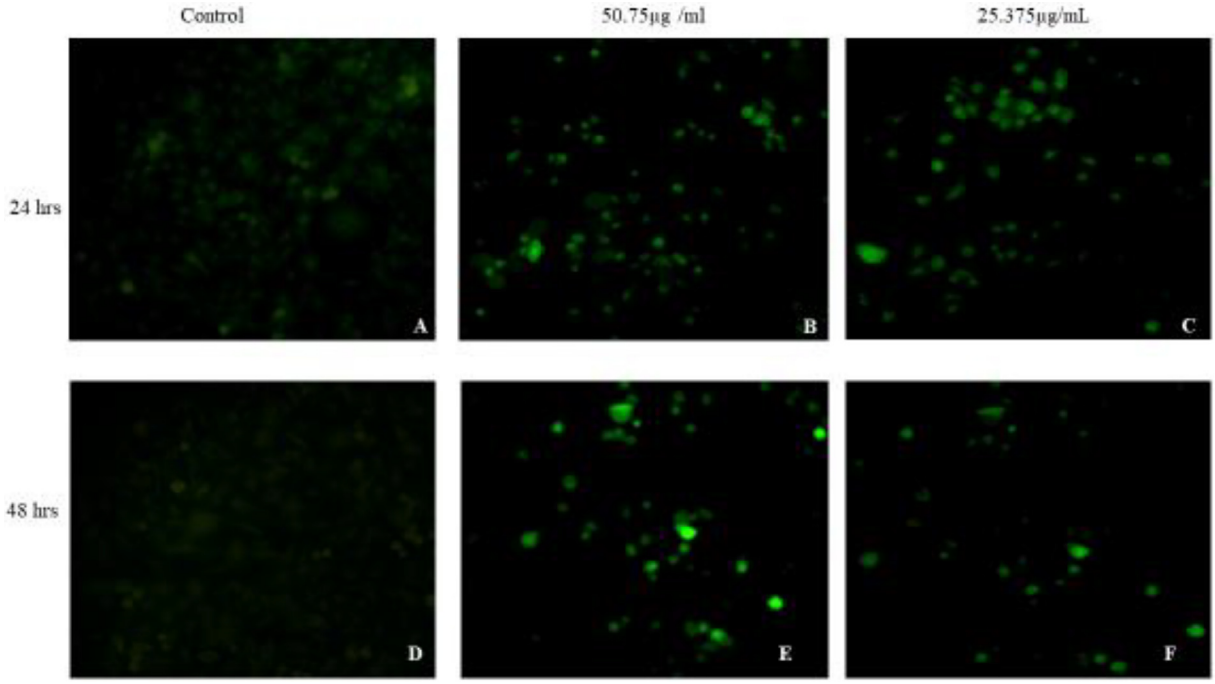

Fig. 2. Photomicrographs of HepG2 cell line stained with DCFH-DA dye. Detection of reactive oxygen species in HepG2 cell line where; (A) & (D) are control cells; (B), (C), (E) & (F) are treated cells.

Table 2A
DDPH free radical inhibition caused by different compounds and extracts.

S. No.	Different Compounds Percentage Inhibition		
	15 µg	25 µg	35 µg
1	31.2590 ± 0.7400	47.9620 ± 0.8100	63.8990 ± 0.8300
2	31.5880 ± 0.3000	41.8890 ± 0.3000	65.5960 ± 0.5000
3	29.8540 ± 0.4900	43.3150 ± 0.6300	67.9840 ± 0.8200
4	29.2570 ± 0.3400	39.0500 ± 0.4100	51.1080 ± 0.7600
5	17.5090 ± 0.4400	32.9700 ± 0.7100	81.3520 ± 0.5700
6	21.2590 ± 0.3000	48.0900 ± 0.5000	61.8830 ± 0.3000
7	21.0340 ± 0.4000	54.7210 ± 0.7000	75.9410 ± 0.5000
8	24.7830 ± 0.5000	47.6870 ± 0.4000	62.5670 ± 0.7000
9	32.1750 ± 0.5600	42.2120 ± 0.6100	61.1450 ± 0.4900
Ascorbic acid	30.7600 ± 0.3000	57.6900 ± 0.2000	79.8900 ± 0.2000

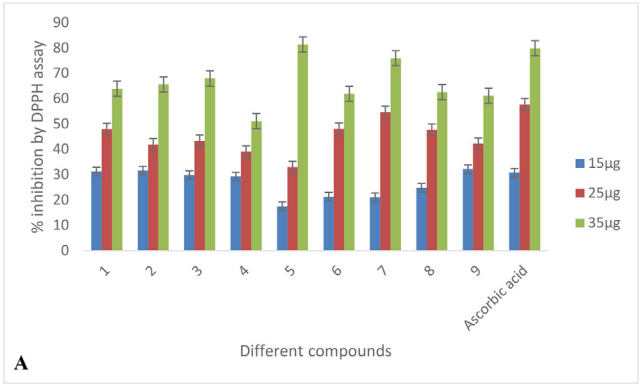

Fig. 3a. DDPH free radical inhibition caused by different compounds.

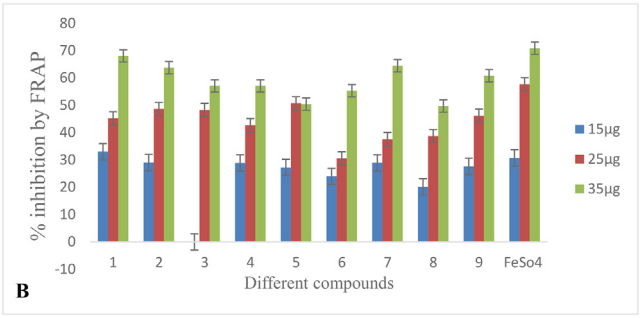

Fig. 3b. Ferric ion scavenging activity of different compounds.

Table 2B
FRAP-ferric ion scavenging activity of different compounds and extracts.

S.No. Different Compounds Percentage Inhibition			
	15 µg	25 µg	35 µg
1	33.0300 ± 0.4300	45.1900 ± 0.8100	68.0700 ± 0.6200
2	29.0400 ± 0.6200	48.6100 ± 0.5500	63.7800 ± 0.2900
3	26.3600 ± 0.6000	48.2900 ± 0.7000	57.0900 ± 0.7000
4	28.8700 ± 0.7500	42.7100 ± 0.5200	57.0900 ± 0.3500
5	27.2700 ± 0.7200	50.7400 ± 0.8600	50.4300 ± 0.2800
6	23.9700 ± 0.3000	30.5800 ± 0.2000	55.2777 ± 0.3000
7	28.9100 ± 0.4000	37.5800 ± 0.7000	64.4400 ± 0.5000
8	20.1610 ± 0.4100	38.7000 ± 0.4600	49.7490 ± 0.7800
9	27.6500 ± 0.5000	46.1900 ± 0.3000	60.8500 ± 0.3000
$FeSO_4$	30.7600 ± 0.3000	57.6900 ± 0.2000	70.8900 ± 0.6000

3.5. Catalase activity

Compounds **1**, **2,** and compound **7** recorded the highest enhancement in enzymatic activities 5212.50 ± 0.61, 5045.83 ± 0. 48, and 5030.83 ± 0.70 respectively (Table 5, Fig. 5B). Compound 3 reported the least activity 3995.83 ± 0.60. Considerably higher catalase enzyme activity was recorded in the compounds, particularly which might have aroused due to a large amount of H_2O_2 generated as the finishing product of SOD catalyzed reaction which has to be neutralized by the optimized treated compounds when compared to control.

Table 3
Antioxidant enzyme activity of the different compounds in terms of IC_{50} and EC_{50} (μg/mL).

S. No.	Different Compounds	DPPH IC_{50} (μg/mL)	FRAP EC50 (μg/mL)
1.	1	14.90	19.44
2.	2	15.44	20.44
3.	3	16.62	23.10
4.	4	15.62	23.52
5.	5	20.61	24.86
6.	6	17.62	26.80
7.	7	15.53	22.46
8.	8	18.08	27.65
9.	9	16.62	26.16
10	Ascorbic acid	**12.66**	–
11.	$FeSO_4$	–	**18.02**

Table 4
Effect of different compounds and extracts on enzymatic activity (SOD).

S. No	Different Compounds	SOD (U/min/gm of FW)
1.	1	427.14 ± 0.52
2.	2	189.80 ± 0.30
3.	3	304.77 ± 0.70
4.	4	225.90 ± 0.53
5.	5	218.60 ± 0.60
6.	6	121.11 ± 0.50
7.	7	206.84 ± 0.20
8.	8	204.10 ± 0.20
9.	9	262.20 ± 0.29

4. Discussion

The reported two new compounds belong to the category of aromatic esters (benzoates) with aliphatic chain and the previous studies already proved that the benzoates are very popular for being used as food preservatives (Franco et al., 2019). Antioxidant potential is one of the prerequisites for food preservation. The isolated two new compounds have shown significant antioxidant potential. The cytotoxicity study suggested that compound **1** was the most potent as compared to (**2**–**9**) on HepG2 cancer cells while almost no effect on A549 cancer cells. Furthermore, (**2**–**9**) did not show cytotoxicity against the human normal liver cell line (WRL-68). Moreover, these cytotoxicity data suggest that compound **1** was the most potent compound isolated from plant extract against HepG2 in comparison to other tested entities in this study. Compound 2 and 7 also exhibited a certain degree of cytotoxicity on HepG2 cell lines. It is also studied previously that alkyl benzoates isolated from red sea sponge *Hyrtios erectus* possess significant

Table 5
Effect of different compounds and extracts on enzymatic activity (CAT).

S. No	Different Compounds	CAT (U/min/gm of FW)
1.	1	5212.50 ± 0.51
2.	2	5045.83 ± 0.28
3.	3	3995.83 ± 0.60
4.	4	4641.66 ± 0.20
5.	5	4212.50 ± 0.50
6.	6	4587.50 ± 0.60
7.	7	5030.83 ± 0.60
8.	8	4108.33 ± 0.50
9.	9	4825.00 ± 0.40

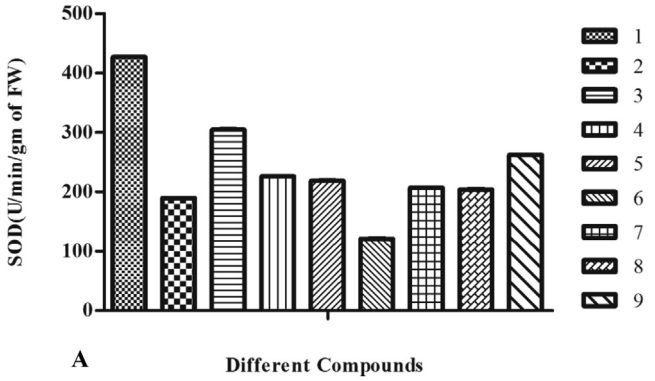

Fig. 5a. Effect of different compounds and extracts on enzymatic activity (SOD).

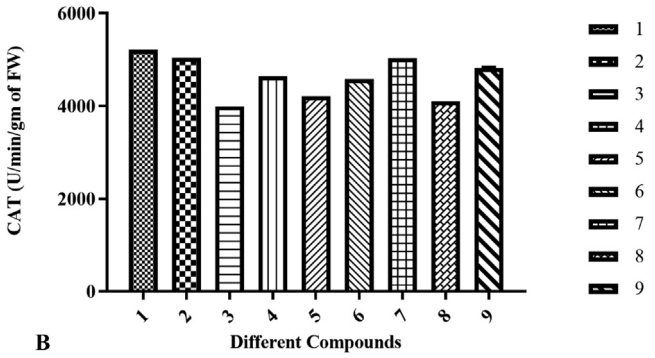

Fig. 5b. Effect of different compounds and extracts on enzymatic activity (CAT).

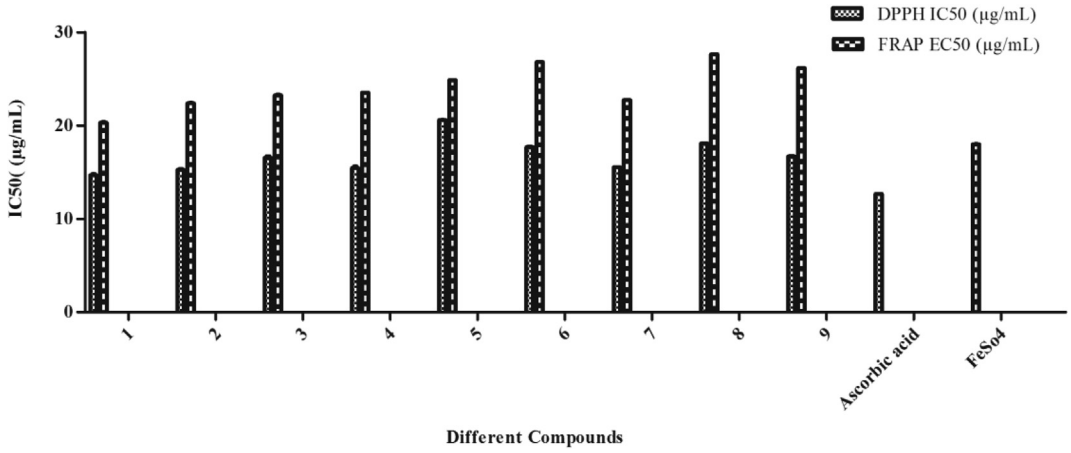

Fig. 4. Antioxidant enzyme activity of the different compounds in terms of IC_{50} and EC_{50} (μg/mL).

cytotoxicity against breast adenocarcinoma (MCF-7) and hepatocellular carcinoma cells (HepG 2) (Hawas et al., 2018).

The generation of some chemically reactive molecules containing ROS takes place endogenously in most of the cells during deisease development, in response to injury and, even in normal course of metabolism. Reactive oxygen species plays an important role in cellular protection and its physiology and contribute to disease initiation, progression and severity. The major physiological functions affected by ROS include proliferation, migration, hypertrophy, differentiation, cytoskeletal dynamics, and metabolism. The excess of ROS leads to its reaction with lipids, proteins, and nucleic acid, thereby altering structural and functional properties of target molecules and leading to tissue dysfunction and injury (Kathy et al., 2016). To control the ROS most of the oxygen is reduced to water, but incomplete reduction of oxygen leads to generation of O_2^-, H_2O_2 and hydroxyl radical. The findings of this experiment suggest that compound 1 significantly affect the ROS production.

Usually the chemical compounds have the role in either potentiation or suppression of the enzymatic activity. Here in this study Compound 1 was found to be the most active compound enhancing the activity of SOD. The reported level of SOD enzyme activity in the compounds might be a defensive response, which could imitate a lower O_2– production or a higher ability for the abolition of O_2–. The variations in the SOD activity in these compounds were too prominent. Therefore, it can be concluded that its presence in all samples suggests that this enzyme may have participated in safeguarding the cells from free superoxide radicals. As far as the antioxidant potential is concerned the FRAP methods reveals that the compounds 1, 2, 7 are most active and exhibited concentration dependent activity but possess lesser reduction power than radical inhibition. DPPH free radical inhibition activity maximally enhanced by compound **1** followed by **2** and **7** and comparable to the standard i.e. ascorbic acid.

5. Conclusion

Extraction and isolation of compounds from the plant were performed through chromatography and two novel compounds were evaluated along with five known compounds. All the isolated compounds and extract of ethyl acetate and *n*-butanol were tested for cytotoxic activity against the growth of HepG2 cancer cells in a dose-dependent and time-dependent manner using an MTT assay to assess cell inhibition. All samples were screened by using an MTT cell viability assay. Compound 1 was the most potent inhibitor of HepG2 cancer cells. It significantly affected the viability of cells till 48 h. The antioxidant activity (DPPH free radical inhibition) of compound and extracts was revealed that the highest inhibition was caused by compound 1 followed by compound 2 and compound 7. The Fe (III) reduction demonstrated that both the treated extracts and compounds had lower reducing ability than the radical inhibiting activity. Compounds 1, 2 and, 7 showed the highest reducing ability estimated by FRAP method. The highest enhancement in SOD activity was reported in compound 1 followed by 2. The over all findings of this study suggest further exploration on both the novel compounds for their biological efficacy or therapeutic advantages.

Acknowledgement

The authors extend their appreciation to Researchers Supporting Project number (RSP-2021/119), King Saud University, Riyadh, Saudi Arabia for supporting and funding this work.

Conflicts of interest

The authors declare no conflicts of interest with respect to research, authorship, and/or publication of this article.

Appendix A. Supplementary data

Supplementary data to this article can be found online at https://doi.org/10.1016/j.jksus.2021.101792.

References

Abbasi, A.M. et al., 2010. J. Ethnopharmacol. 128, 322–335. https://doi.org/10.1016/j.jep.2010.01.052.
Aebi, H., 1984. Methods Enzymol. 1984 (105), 121–126. https://doi.org/10.1016/s0076-6879(84)05016-3.
Anonymous, 2004. The Ayurvedic Pharmacopoeia of India, Part-I, vol.-IV, Government of India, Ministry of Health and Family Welfare, Department of Health, New Delhi.
Benzie, I.F., Strain, J.J., 1996. Anal Biochemis. 239 (1), 70–76. https://doi.org/10.1006/abio.1996.0292.
Blois, M.S., 1958. Nature. 29, 1199–1200. https://doi.org/10.1038/1811199a0.
Fraga, D., et al., 2017. Real-time PCR: Current protocols essential laboratory techniques, 2008, (1), 10-3. https://doi.org/10.1002/9780470089941.et1003s00
Franco, R. et al., 2019. Antioxidants 8, 542–554. https://doi.org/10.3390/antiox8110542.
Gaur, R.D., 1999. Flora of District Garhwal, North Western Himalaya (with ethnobotanical notes). Transmedia, Srinagar, Uttarakhand, India.
Ghali, W. et al., 2014. Cancer Metabol. 2 (Suppl. 1), 21. https://doi.org/10.1186/2049-3002-2-S1-P21.
Giannopolitis, C.N., Ries, S.K., 1977. Plant Physiol. 59 (2), 309–314. https://doi.org/10.1104/pp.59.2.309.
Guo, T. et al., 2017. Nat. Prod. Res. 31 (1), 16–21. https://doi.org/10.1080/14786419.2016.1205064.
Hawas, U.W. et al., 2018. Nat. Prod. Res., 32, 12.: 1369-74. https://doi.org/10.1080/14786419.2017.1344662
Kalia, N.K. et al., 1999. J Nat Prod. 62 (6), 311–312. https://doi.org/10.1021/np980224j.
Karimi, E. et al., 2010. Molecules 15 (9), 6244–6256. https://doi.org/10.3390/molecules15096244.
Kathy, et. al., 2016. Circ. Res. 119 (5): doi:e39-e75. 10.1161/RES0000000000000110; PMID: 27418630.
Khazaei, S. et al., 2017. BMC Complement. Altern. Med. 17 (1), 104–115. https://doi.org/10.1186/s12906-017-1594-6.
Mukherjee, S.P., Choudhuri, M.A., 1983. Physiol. Plantarum 58, 166–170. https://doi.org/10.1111/j.1399-3054.1983.tb04162.x.
Mushtaq, M.N. et al., 2019. Phytomed. 53, 163–170. https://doi.org/10.1016/j.phymed.2018.09.020.
Nooreen, Z. et al., 2017a. Biomed. Pharmacother. 89, 366–375. https://doi.org/10.1016/j.biopha.2017.02.040.
Nooreen, Z. et al., 2017b. Nat. Prod. Res. 33 (5), 665–672. https://doi.org/10.1080/14786419.2017.1405404.
Phuyal, N. et al., 2018. J. Ethnopharmacol. 229, 326–341. https://doi.org/10.1016/j.jep.2018.08.010.
Siddiqui, S., 2015. Cell Prolifera. 48 (4), 443–454. https://doi.org/10.1111/cpr.12195.
Singh, T.P., Singh, O.M., 2011. Indian J. Nat. Prod. Res. 2 (3), 275–285 http://hdl.handle.net/123456789/12730.